



Enantioselective (8+3) Cycloadditions by Activation of Donor–Acceptor Cyclopropanes Employing Chiral Brønsted Base Catalysis

David A. McLeod, Mathias Kirk Thøgersen, Casper Larsen Barløse, Mette Louise Skipper, Erlaitz Basabe Obregón, and Karl Anker Jørgensen*

Abstract: A novel enantioselective (8+3) cycloaddition between donor–acceptor cyclopropanes and heptafulvenoids catalysed by a chiral bifunctional Brønsted base is described. Importantly, the reaction, which leverages an anionic activation strategy, is divergent from prototypical Lewis-acid activation protocols. A series of cyclopropylketones react with tropones affording the desired (8+3) cycloadducts in high yield and enantiomeric excess. For barbiturate substituted heptafulvenes, the (8+3) cycloaddition with cyclopropylketones proceeds in good yield, excellent diastereoselectivity and high enantiomeric excess. The experimental work is supported by DFT calculations, which indicate that the bifunctional organocatalyst activates both the donor–acceptor cyclopropane and tropones; the reaction proceeds in a step-wise manner with the ring-closure being the stereo-determining step.

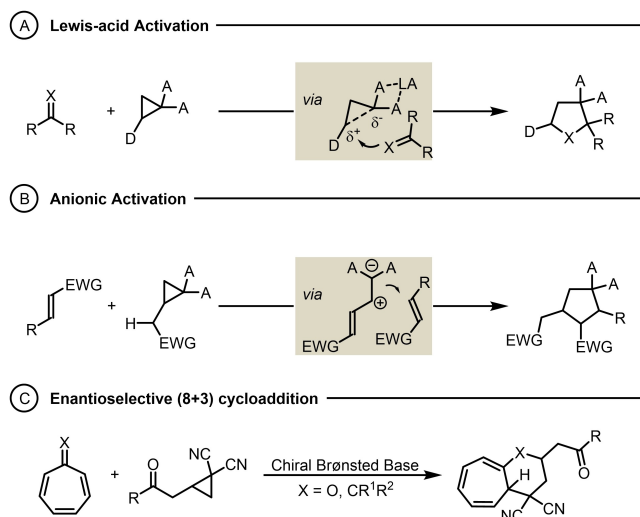


Figure 1. A) An example of a classical (3+2) cycloaddition employing Lewis-acid activation of a donor–acceptor cyclopropane. B) A nucleophilic (anionic) activation strategy for (3+2) cycloadditions. C) The envisioned organocatalytic enantioselective (8+3) cycloaddition.

Introduction

The field of donor–acceptor cyclopropane chemistry, while well established, has seen a renaissance in recent years as new and innovative activation strategies have expanded the frontiers of their chemistry.^[1] The high reactivity of donor–acceptor cyclopropanes—owing to the inherent strain in the cyclopropane ring and the push–pull effect of the vicinal donor–acceptor substituents resulting in significant C–C bond polarisation—makes them versatile synthetic intermediates in organic synthesis.^[2] Although the synergistic push–pull effect can facilitate the strain-driven ring opening, Lewis acids are typically employed to increase the electrophilicity of the system, thereby further promoting reactivity through coordinating an acceptor group such as an ester (Figure 1A).^[1] In contrast, nucleophilic activation strategies

in which the reaction is promoted through activation of the donor group are rare,^[3,4] and include only two examples of cycloadditions (Figure 1B).^[4c,d] Therefore, while advances in electrophilic activation have driven the resurgence of donor–acceptor cyclopropane chemistry, development of nucleophilic activation strategies has lagged behind.

Cycloadditions are innately complexity generating and atom economical, and donor–acceptor cyclopropanes have been extensively applied as 1,3-zwitterions in (3+2),^[5] (3+3),^[6] and (3+4)^[7] cycloadditions. Much less common are (8+3) cycloadditions of donor–acceptor cyclopropanes,^[8] with only two reports. Rivero et al. reported that donor–acceptor aminocyclopropanes react with substituted tropones in the presence of a catalytic amount of SnCl₄ to give (8+3) cycloadducts.^[8a] Concurrently, Tejero et al. published a nickel-catalysed (8+3) cycloaddition of 1,1-cyclopropane diesters and tropones; notably, only a single chiral entry has been demonstrated with moderate yield and enantioselectivity.^[8b] These Lewis acid activation strategies leverage the ability of tropones to react as a nucleophilic 8π-component. We envisaged the antipode strategy, wherein cycloaddition commences when a suitable donor–acceptor cyclopropane, activated by a chiral Brønsted base, nucleophilically adds to a suitable heptafulvenoid—the cycloaddi-

[*] Dr. D. A. McLeod, Dr. M. K. Thøgersen, Dr. C. L. Barløse, M. L. Skipper, E. B. Obregón, Prof. Dr. K. A. Jørgensen
Department of Chemistry, Aarhus University
8000 Aarhus C (Denmark)
E-mail: kaj@chem.au.dk

© 2022 The Authors. Angewandte Chemie International Edition published by Wiley-VCH GmbH. This is an open access article under the terms of the Creative Commons Attribution Non-Commercial NoDerivs License, which permits use and distribution in any medium, provided the original work is properly cited, the use is non-commercial and no modifications or adaptations are made.

tion would then be completed through an (oxa)-Michael reaction onto the α,β -unsaturated ketone (Figure 1C).

Results and Discussion

The desired (8+3) cycloaddition reaction of racemic cyclopropylmethylketone **1a** with tropone **2a** proceeds in the presence of a catalytic amount of Et₃N to give the cycloadduct **4aa** in 61 % yield. In the absence of the base, no product formation was observed. Interestingly, **4aa**, the product of post-cycloaddition 1,3-*H* sigmatropic rearrangement, was formed as the sole observable product—no trace of the initially formed cycloadduct was ever observed. Encouraged by these results, a number of different families of optically active Brønsted bases were tested as catalysts (see Table 1 and Supporting Information).

The bifunctional Takemoto catalyst^[9] **3a** gave the most promising enantioselectivity of the initially tested bases (Table 1, entry 1). Lowering the reaction temperature to 4 °C led to a significant decrease in the rate of reaction, but increased the enantioselectivity to 84 % *ee* (entry 2). Further cooling of the reaction proved impractical albeit the product was obtained with a slight improvement in enantioselectivity

(entry 3). A survey of solvents revealed that 1,1,1-trichloroethane (TCE) was the best choice with respect to reactivity and yield (entries 2, 4–6), and furnished the product with only slightly diminished enantioselectivity. Lowering the temperature increased the enantioselectivity back up to 81 % *ee* (entry 7); however, further attempts using catalyst **3a** did not improve the enantioselectivity (see Supporting Information).

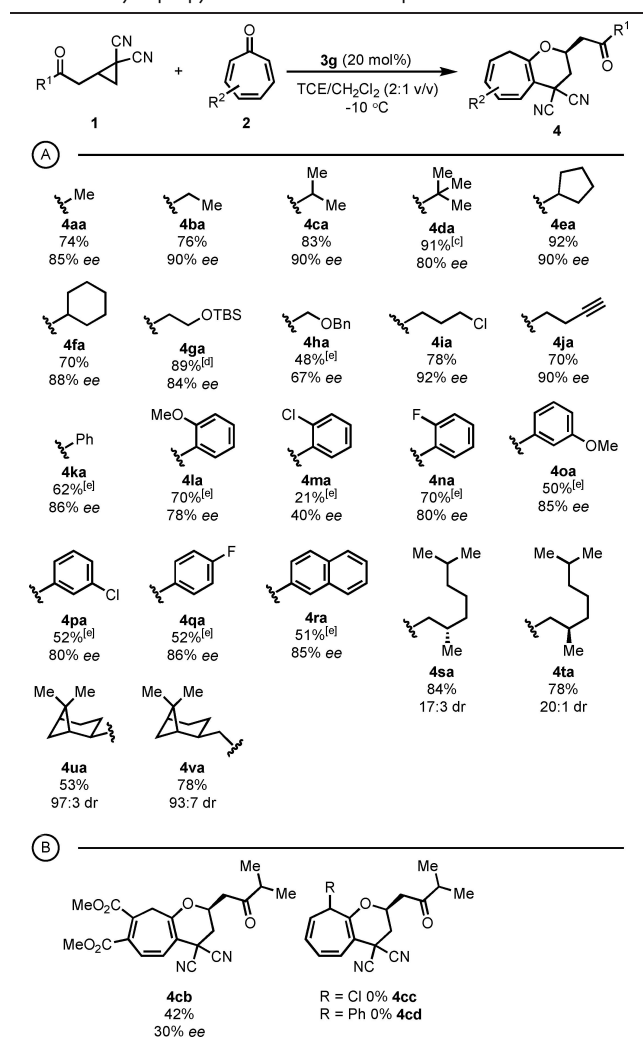
Considering the significant effects reported by changing the tertiary amine moiety of the catalyst,^[10] we focused our attention on exploring alternative groups there first. Implementing a *N*-pyrrolidinyl moiety as the Brønsted base (**3b**) led to a more active catalyst, but with decreased enantioselectivity. Increasing the ring size to an *N*-piperidyl group (**3c**) resulted in a significant decrease in both catalyst reactivity and enantioselectivity. The less basic *N*-morpholinyl catalyst (**3d**) showed no reactivity (entry 10). As it became apparent the *N,N*-dimethylamino group was key to achieving high enantioselectivity, we next centred our attention to the hydrogen-bond donor moiety. Varying the substitution pattern of the aromatic ring led to drastic differences in catalyst activity with selected examples shown in Table 1 (see Supporting Information). The *p*-methoxy catalyst **3e** displayed significantly lower reactivity with a similar enantioselectivity (entry 11). Introduction of a trifluoromethyl substituent in the *para*-position (**3f**) led to a modest increase in the enantioselectivity, but still displayed slightly reduced catalyst activity (entry 12). It became apparent from screening catalysts that the interaction between the catalyst and tropone is crucial for good reactivity; therefore, we reasoned that introduction of a strongly electron-withdrawing moiety, to increase the acidity of the thiourea hydrogen, would lead to increased catalyst performance.^[11] Gratifyingly, installation of a nitro group in the *para*-position led to slightly increased reactivity and enantioselectivity (entry 13); fluorinated catalyst **3h** induced similar enantioselectivity as **3g** (entry 14), however, it displayed slightly lower reactivity, particularly with more bulky substrates (see below). After extensive optimisation of the system, the final conditions employed catalyst **3g** in a trichloroethane/dichloromethane binary solvent mixture at –10 °C (entry 15).

With the optimised conditions in hand, we next investigated the scope of the (8+3) cycloaddition employing cyclopropylketones **1a–v**. Aliphatic substituents (**1a–j**) were well tolerated and furnished the corresponding cycloadducts **4aa–ja** in good yield and enantioselectivity (Table 2A). The reaction displayed a noticeable retardation with increasing steric bulk of the α -substituent, as such the entry **4da** bearing a *tert*-butyl group was run at 4 °C. Substrates **1g** and **1h** bearing oxygen-containing functional groups proved intolerant of catalyst **3g**, however, catalyst **3h** was a suitable replacement furnishing **4ga** in 89 % yield and 84 % *ee*; benzyloxycyclopropane **1h** was still too reactive and so required further cooling to –25 °C. Aromatic substrates **1k–r** were also quite reactive and so required the same conditions as **1h**, but gratifyingly, cycloadducts **4ka–ra** were obtained in generally reasonable yield and high enantioselectivity.

Table 1: Optimization of the reaction conditions.^[a]

Entry	Catalyst	Solvent	T [°C]	Yield [%] ^[b]	<i>ee</i> [%] ^[c]
1	3a	CH ₂ Cl ₂	23	61	78
2 ^[d]	3a	CH ₂ Cl ₂	4	52	84
3 ^[e]	3a	CH ₂ Cl ₂	–25	12	88
4 ^[d]	3a	PhMe	4	36	64
5 ^[f]	3a	MTBE	4	27	70
6	3a	TCE	4	70	78
7	3a	TCE	–25	62	81
8	3b	TCE	–25	72	72
9	3c	TCE	–25	17	19
10	3d	TCE	–25	0	ND
11	3e	TCE	–25	15	79
12	3f	TCE	–25	61	86
13	3g	TCE	–25	65	87
14 ^[d]	3h	TCE	–25	63	86
15	3g	TCE/CH ₂ Cl ₂ (2:1)	–10	74	85

[a] Unless otherwise noted, the reactions were performed with **1a** (0.075 mmol) and **2a** (0.05 mmol) with **3a–h** (20 mol%) in solvent (0.3 mL) for 36 h. [b] Yield of isolated product. [c] Determined by UPC² on a chiral stationary phase. [d] Reaction time of 48 h. [e] Reaction time of 7 d. [f] Reaction time of 60 h. MTBE = methyl *tert*-butyl ether, TCE = 1,1,1-trichloroethane.

Table 2: Reaction scope of the Brønsted base catalysed (8+3) cycloaddition of cyclopropylketones **1a–v** and tropones **2a–d**.^[a,b]

[a] Reaction conditions: **1** (0.15 mmol), **2** (0.10 mmol), **3g** (20 mol%), TCE/CH₂Cl₂ (2:1 v/v), −10 °C. [b] Yield of isolated product; enantiomeric excess (*ee*) was determined by UPC² on a chiral stationary phase. [c] Reaction performed at 4 °C. [d] Catalyst **3h** (20 mol%) used instead. [e] Reaction conditions: **1** (0.10 mmol), **2** (0.40 mmol), **3h** (20 mol%) TCE/CH₂Cl₂ (2:1 v/v), −25 °C.

Chiral starting materials **1s–v** also performed well in the reaction. Importantly, the formed stereogenic centre is predominantly controlled by the catalyst. Citronellol-derived cyclopropanes **1s** and **1t** cleanly furnished the corresponding cycloadducts **4sa** and **4ta** in excellent yield and nearly identical diastereoselectivity—only a slight stereochemical mismatch was observed. Cyclopropanes **1u** and **1v** (derived from monoterpenes (1*R*)-myrtenol and (1*R*)-nopol, respectively) also afforded the desired cycloheptapyran products **4ua** and **4va** in reasonably good yield and diastereoselectivity, however, the increased steric bulk presented by **1u** led to retardation of the rate of reaction and consequently a diminished isolated yield.

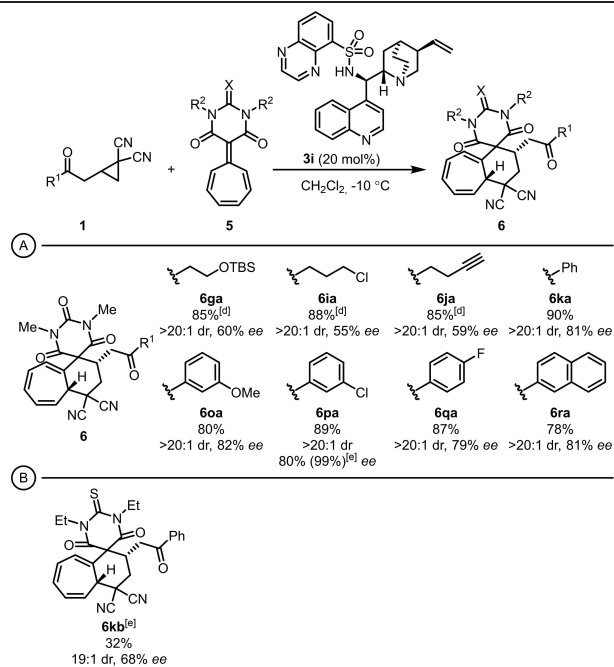
The reaction was next attempted with functionalised tropones **2b–d** (Table 2B). Troponone **2b** underwent the

desired (8+3) cycloaddition with cyclopropane **1c** to give cycloheptapyran **4cb** in moderate yield and enantioselectivity. Unfortunately, tropones **2c,d** featuring substituents in the 2-position displayed no reaction, even at room temperature.

The absolute configuration of the products **4** was assigned on the basis of the X-ray crystal structure of the cycloadduct **4aa** derivatised as the 4-bromo-2-nitrohydrazone (see Supporting Information).

Gratifyingly, heptafulvenes **5** were also found to participate in the desired (8+3) cycloaddition, furnishing cycloadducts **6** (Table 3). However, whereas the bifunctional Takemoto scaffold proved efficient inducing enantioselectivity in reactions involving tropones **2**, it was only weakly enantioselective in reactions with heptafulvenes **5**. Exhaustive reaction screening led to identification of the cinchona alkaloid derived catalyst **3i** which displayed a high degree of enantioselectivity (see Supporting Information for full catalyst screening). Interestingly, the (8+3) cycloadducts of heptafulvenes showed no propensity to undergo isomerisation of the triene, and were thus isolated with both stereocentres intact.

Investigation of the reaction of barbiturate heptafulvene **5a** with aliphatic cyclopropanes **1g,i,j** catalysed by **3i** afforded cycloadducts **6ga**, **6ia** and **6ja**, respectively, in excellent yield and diastereoselectivity, and reasonable enantioselectivity (Table 3A). The more reactive aromatic cyclopropanes **1k,o–r** also performed well, producing cyclo-

Table 3: Reaction scope of the Brønsted base catalysed (8+3) cycloaddition of cyclopropylketones **1** and barbiturate heptafulvenes **5**.^[a,b,c]

[a] Reaction conditions: **1** (0.15 mmol), **5** (0.1 mmol), **3i** (20 mol%), TCE/CH₂Cl₂ (2:1 v/v), −10 °C. [b] Yield of isolated product; *ee* was determined by UPC² on a chiral stationary phase. [c] Diastereomeric ratio (dr) was determined by ¹H NMR spectroscopy on isolated products. [d] Reaction performed at rt. [e] Reaction performed at 4 °C.

adducts **6k**, **o–r** with similarly high yields, but with improved enantioselectivity. Interestingly, the enantioselectivity of **6pa** could be improved by crystallisation of the racemic product from the bulk sample, furnishing **6pa** with $\geq 99\%$ *ee*. Investigation of various heptafulvenes identified the thiobarbiturate **5b** which also furnished the desired (8+3) cycloadducts, albeit in diminished yield and stereoselectivity (Table 3B). Cyanoester- and dicyano-heptafulvenes proved mostly unreactive under the reaction conditions.

The absolute configuration of the products **6** was assigned on the basis of the X-ray crystal structure of the cycloadduct **6pa** (see Supporting Information). The different catalyst chemotype employed for the heptafulvenes led to a different absolute configuration than for products **4**, which used the Takemoto-type catalysts. This reaction pathway was, however, not investigated.

To gain more insight into the origin of the stereoselectivity of the above process, a computational density functional theory (DFT) study was carried out. All geometries were optimised using the ω B97xD functional and Jensen's pcseg-1 basis set with the SMD solvent continuum in dichloromethane.^[12] The single-point energies of the optimised structures were then calculated at the PBE0-D3(BJ)/6-311++G(2d,2p)/SMD(CH₂Cl₂) level of theory.^[13] All calculations were performed by using the Gaussian09 or Gaussian16 software package.^[14] The free energies presented and discussed were calculated by applying the free energy correction from the ω B97xD/pcseg-1/SMD(CH₂Cl₂) to the single-point energies (see Supporting Information for full computational description).

The substrate-catalyst H-bond pattern in the transition state (TS) corresponding to the first C–C bond forming step was thoroughly investigated (Figure 2). While several computational studies of reactions involving Takemoto-type catalysts have been reported, few concern cycloadditions.^[15,16] It was expected that the energy differences between the possible H-bonding interactions would be low, enabling a high degree of mobility in the coordination sphere of the catalyst.^[17]

Among the several possible ternary nucleophile–electrophile H-bond complexes, binding mode D (BMD) is preferred, wherein the deprotonated nucleophile, directed by the ionic NH⁺⋯NC interaction, attacks tropone—which is activated by the bidentate interaction of the thiourea N–Hs, as proposed by Takemoto et al.^[15f] The other binding modes (BMA–BMC) were shown to exhibit significantly higher energies, likely as a consequence of the ionic species stabilised by *non-ionic* interactions. Surprisingly, little facial selectivity was found for the first step for BMD, as the difference in TS energies for the (*R*)- and (*S*)-pathways are near *iso*-energetic ($\Delta\Delta G^\ddagger = 0.2$ kcal mol⁻¹), leading to a 58:42 ratio of (*R*)- and (*S*)-intermediates **Int-I** (Figures 3 and 4). Geometries for both TSs allow for good alignment of key ionic interactions while also favourable activation of the tropone by the amide protons and π - π /Van der Waals (VdW) interactions can be observed between the *p*-NO₂-C₆H₄-moiety of the catalyst with the α,β -unsaturated ketone of the nucleophile in the non-covalent interactions plot (NCI-plot, see Supporting Information).^[18]

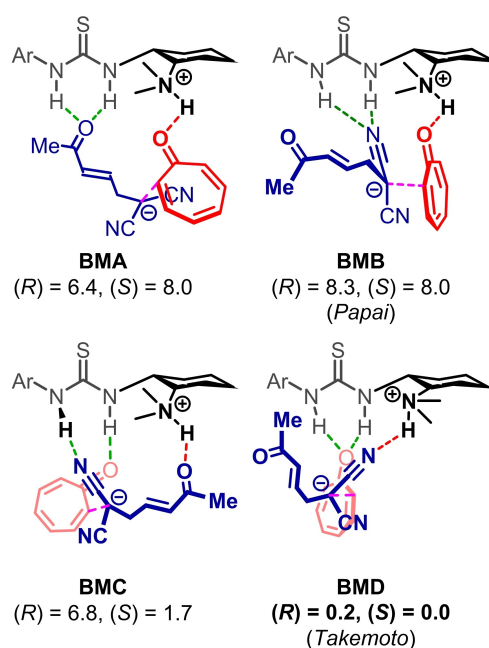


Figure 2. Four possible binding modes and their corresponding lowest TS-energies for the (*R*)- and (*S*)-pathway for the first bond formation. Calculated at the PBE0-D3(BJ)/6-311++G(2d,2p)/SMD(CH₂Cl₂)/ ω B97xD/pcseg-1/SMD(CH₂Cl₂) level of theory. --- indicates the TS bond while - - - indicates hydrogen bond interactions and - - - indicate ionic interactions. Gibbs free energies are in kcal mol⁻¹ and are relative to the lowest TS energy for the first bond formation. Ar = *p*-NO₂-C₆H₄.

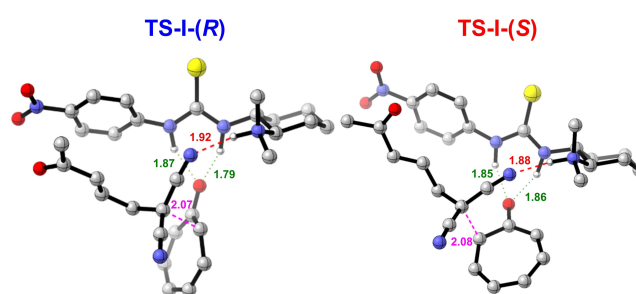


Figure 3. Enantiomeric TSSs corresponding to the first C–C bond forming event. Left: TS for the (*S*)-pathway. Right: TS for the (*R*)-pathway. --- indicates the TS bond while - - - indicates ionic interactions and indicates hydrogen bond interactions. Distances are in Ångströms and C–H hydrogens are omitted for clarity.

The computed reaction profile of the process between cyclopropylmethylketone **1a** and tropone **2a** is shown in Figure 4, which shows the relative free energies in CH₂Cl₂ solution. Although the initial C–C bond formation occurs with poor enantioselectivity, the ring-closing oxa-Michael reaction, facilitated by the catalyst, was found to be highly diastereoselective for the (*R*)-stereocentre (Figure 5). Ring closure from the (*R*)- and (*S*)-intermediates proceeds preferentially via binding mode C (BMC) through a boat-conformation stabilised by the catalyst, **TS-II-(RR)** and **TS-II-(SR)** respectively, with the latter being the lowest energy TS. The α,β -unsaturated ketone is activated through hydro-

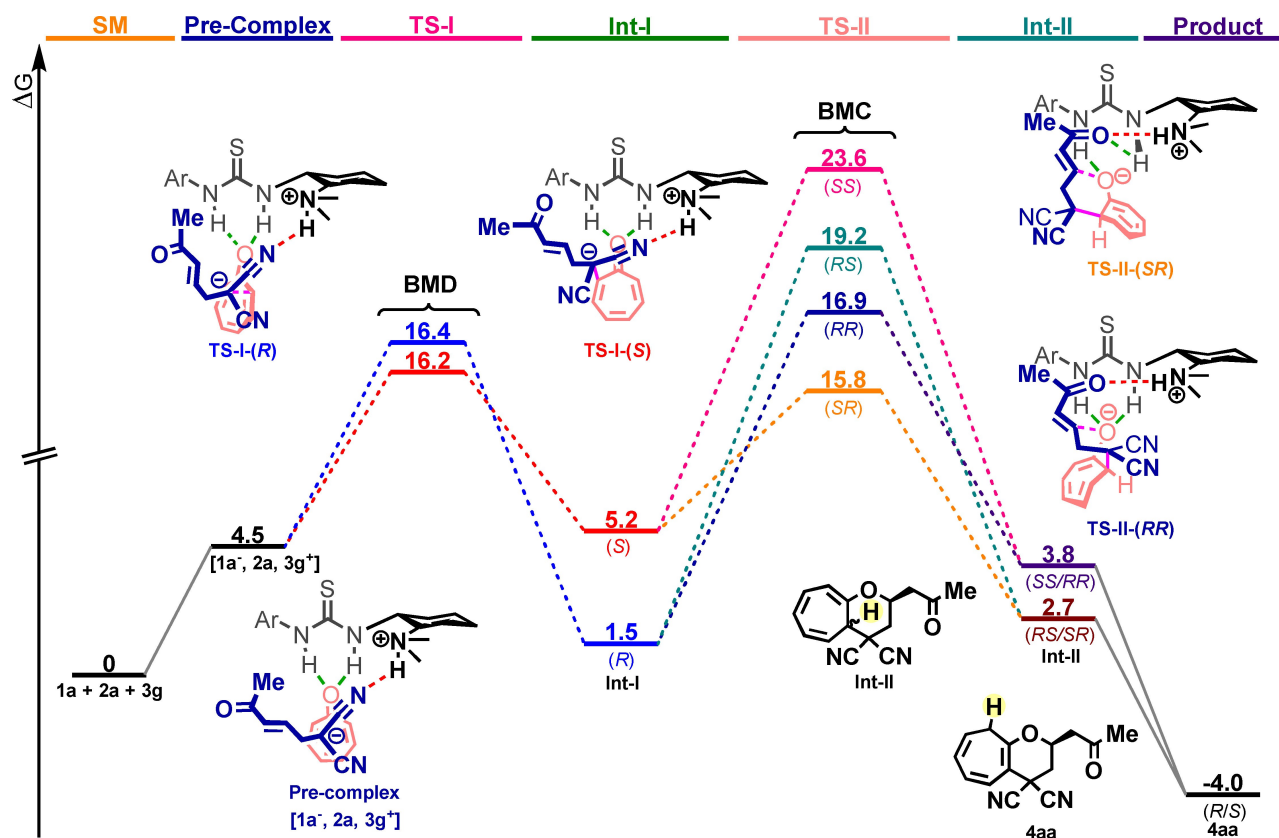


Figure 4. An overview of the reaction pathway for the formation of **4aa** and *ent*-**4aa**. Red and blue dotted lines show the pathway for enantioselective first bond formation while the orange, navy blue, pink and green dotted lines show the diastereoselective pathways for the second bond formation. Grey lines indicate unexplored pathways only connected by its products. All energies are Gibbs free energy in kcal mol⁻¹ and are relative to the sum of the energies of the starting materials **1a**, **2a** and **3g**. Calculated at the PBE0-D3(BJ)/6-311++G(2d,2p)/SMD(CH₂Cl₂)/ωB97xD/pcseg-1/SMD(CH₂Cl₂) level of theory.

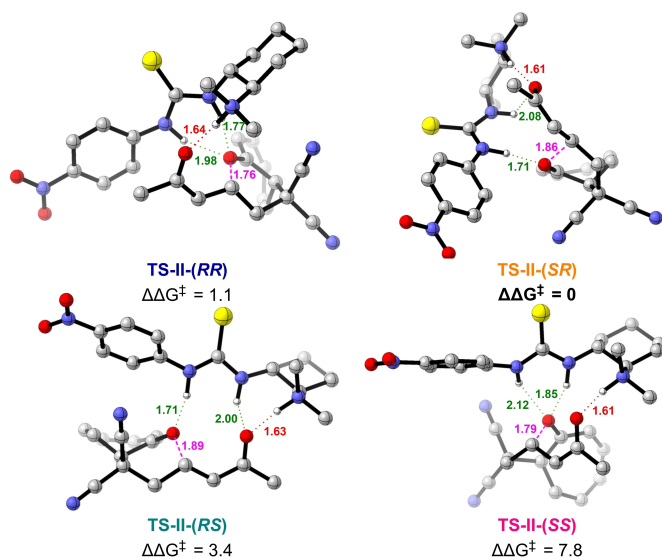


Figure 5. --- indicates the TS bond while indicates ionic-hydrogen bond interactions and indicates hydrogen bond interactions. Distances are in Ångströms and C-H hydrogens are omitted for clarity. Gibbs free energies are in kcal mol⁻¹ and are relative to the lowest TS energy for the second bond formation.

gen bonding of the ketone to the alkyllammonium moiety of the catalyst, stabilising developing charge (see Supporting Information for NCI-plots). **TS-II-(RS)** and **TS-II-(SR)** also possess additional interactions between the ketone and the thiourea. The nucleophilic oxygen of tropone is stabilised by the acidic amide protons of the catalyst. The two lowest energy TSs leading to the (*S*)-stereocentre, **TS-II-(RS)** and **TS-II-(SS)**, are 2.3 kcal mol⁻¹ and 6.7 kcal mol⁻¹ higher in energy respectively. Thereafter, a post-cycloaddition *1,3-H* sigmatropic rearrangement occurs resulting in loss of stereochemical information from the ring junction furnishing the isolated final product with good enantioselectivity (see Supporting Information). The driving force for triene isomerisation can be rationalised by the formation of a tetrasubstituted olefin which gives a thermodynamically more stable product. The differences in TS energies for the first and second bond formation leads to a **Int-II** distribution of 42:57:1:0 with stereochemistry **RR:SR:RS:SS**. After isomerisation this ratio is translated into a calculated 98% *ee* of (*R*)-**4aa**, in accordance with the experimentally observed 85% *ee*.

Conclusion

In conclusion, an enantioselective (8+3) cycloaddition of donor-acceptor cyclopropanes and heptafulvenoids was developed using optically active bifunctional Brønsted-base catalysts. The reaction displayed a broad substrate scope and furnished the desired cycloadducts with good enantioselectivity. Reactions of chiral starting materials indicate the reaction is predominantly controlled by the bifunctional organocatalyst. Importantly, the reaction leverages an anionic/nucleophilic cyclopropane activation strategy—an area which remains severely under-developed. The experimental results are supported by DFT calculations demonstrating the necessity of the bifunctional catalyst and offer important insight into the origin of diastereo- and enantioselectivity for these complex reactions.

Acknowledgements

K.A.J. thanks Villum Investigator grant (no. 25867 and Aarhus University for financial support. The numerical results presented in this work were obtained at the Centre for Scientific Computing, Aarhus (<http://phys.au.dk/for-skning/cscaa/>).

Conflict of Interest

The authors declare no conflict of interest.

Data Availability Statement

The data that support the findings of this study are available in the Supporting Information of this article.

Keywords: Brønsted Base · Cyclopropanes · Heptafulvenoids · Organocatalysis · Tropones

- [1] For a summary of activation modes, see: a) S. Kolb, M. Petzold, F. Brandt, P. G. Jones, C. R. Jacob, D. B. Werz, *Angew. Chem. Int. Ed.* **2021**, *60*, 15928–15934; *Angew. Chem.* **2021**, *133*, 16064–16070, and references therein; b) T. F. Schneider, J. Kaschel, D. B. Werz, *Angew. Chem. Int. Ed.* **2014**, *53*, 5504–5523; *Angew. Chem.* **2014**, *126*, 5608–5628.
- [2] a) H.-U. Reissig, R. Zimmer, *Chem. Rev.* **2003**, *103*, 1151–1196; b) K. Ghosh, S. Das, *Org. Biomol. Chem.* **2021**, *19*, 965–982.
- [3] For oxyanion-induced reactions, see: a) E. Wenkert, R. A. Mueller, E. J. Reardon, Jr., S. S. Sathe, D. J. Scharf, G. Tosi, *J. Am. Chem. Soc.* **1970**, *92*, 7428–7436; b) E. Wenkert, *Acc. Chem. Res.* **1980**, *13*, 27–31; c) H.-U. Reissig, E. Hirsch, *Angew. Chem. Int. Ed. Engl.* **1980**, *19*, 813–814; *Angew. Chem.* **1980**, *92*, 839–840; d) H.-U. Reissig, *Tetrahedron Lett.* **1981**, *22*, 2981–2984; e) E. Kunkel, I. Reichelt, H.-U. Reissig, *Liebigs Ann. Chem.* **1984**, 802–819; f) E. L. Grimm, H.-U. Reissig, *J. Org. Chem.* **1985**, *50*, 242–244; g) C. Brückner, H.-U. Reissig, *Angew. Chem. Int. Ed. Engl.* **1985**, *24*, 588–589; *Angew. Chem.* **1985**, *97*, 578–579; h) J. P. Marino, E. Laborde, *J. Am. Chem. Soc.* **1985**, *107*, 734–735; i) Q.-Q. Cheng, J. Yedoyan, H. Arman, M. F. Doyle, *Angew. Chem. Int. Ed.* **2016**, *55*, 5573–5576; *Angew. Chem.* **2016**, *128*, 5663–5666.
- [4] For carbanion-induced reactions, see: a) C. Stirling, *Chem. Rev.* **1978**, *78*, 517–567; b) A. Tomazic, E. Ghera, *Tetrahedron Lett.* **1981**, *22*, 4349–4352; c) I. Reichelt, H.-U. Reissig, *Liebigs Ann. Chem.* **1984**, 828–830; d) M. Sasaki, Y. Kondo, T. Nishio, K. Takeda, *Org. Lett.* **2016**, *18*, 3858–3861; e) J. Blom, A. Vidal-Albalat, J. Jørgensen, C. L. Barløse, K. S. Jessen, M. V. Iversen, K. A. Jørgensen, *Angew. Chem. Int. Ed.* **2017**, *56*, 11831–11835; *Angew. Chem.* **2017**, *129*, 11993–11997.
- [5] For examples of (3+2) cycloadditions of donor-acceptor cyclopropanes, see: a) G. A. Oliver, M. N. Loch, A. U. Augustin, P. Steinbach, M. Sharique, U. K. Tambar, P. G. Jones, C. Bannwarth, D. B. Werz, *Angew. Chem. Int. Ed.* **2021**, *60*, 25825–25831; *Angew. Chem.* **2021**, *133*, 26029–26035, and the references therein.
- [6] For examples of (3+3) cycloadditions of donor-acceptor cyclopropanes, see: a) M. Petzold, P. G. Jones, D. B. Werz, *Angew. Chem. Int. Ed.* **2019**, *58*, 6225–6229; *Angew. Chem.* **2019**, *131*, 6291–6295; b) P. S. Dhote, C. V. Ramana, *Org. Lett.* **2019**, *21*, 6221–6224; c) A. O. Chagarovskiy, V. S. Vasin, V. V. Kuznetsov, O. A. Ivanova, V. B. Rybakov, A. N. Shumsky, N. N. Makhova, I. V. Trushkov, *Angew. Chem. Int. Ed.* **2018**, *57*, 10338–10342; *Angew. Chem.* **2018**, *130*, 10495–10499; d) P.-W. Xu, J.-K. Liu, L. Shen, Z.-Y. Cao, X.-L. Zhao, J. Yan, J. Zhou, *Nat. Commun.* **2017**, *8*, 1619; e) T. Chidley, N. Vemula, C. A. Carson, M. A. Kerr, B. L. Pagenkopf, *Org. Lett.* **2016**, *18*, 2922–2925; f) L. K. B. Garve, M. Petzold, P. G. Jones, D. B. Werz, *Org. Lett.* **2016**, *18*, 564–567; g) C. M. Braun, E. A. Congdon, K. A. Nolin, *J. Org. Chem.* **2015**, *80*, 1979–1984; h) H. Liu, C. Yuan, Y. Wu, Y. Xiao, H. Guo, *Org. Lett.* **2015**, *17*, 4220–4223.
- [7] For examples of (3+4) cycloadditions of donor-acceptor cyclopropanes, see: a) A. U. Augustin, J. L. Merz, P. G. Jones, G. Mlostoń, D. B. Werz, *Org. Lett.* **2019**, *21*, 9405–9409; b) Z.-H. Wang, H.-H. Zhang, D.-M. Wang, P.-F. Xu, Y.-C. Luo, *Chem. Commun.* **2017**, *53*, 8521–8524; c) L. K. B. Garve, M. Pawliczek, J. Wallbaum, P. G. Jones, D. B. Werz, *Chem. Eur. J.* **2016**, *22*, 521–525; d) H. Xu, J.-L. Hu, L. Wang, S. Liao, Y. Tang, *J. Am. Chem. Soc.* **2015**, *137*, 8006–8009; e) O. A. Ivanova, E. M. Budynina, Y. K. Grishin, I. V. Trushkov, P. V. Verteletskii, *Angew. Chem. Int. Ed.* **2008**, *47*, 1107–1110; *Angew. Chem.* **2008**, *120*, 1123–1126.
- [8] a) A. R. Rivero, I. Fernández, M. Á. Sierra, *Org. Lett.* **2013**, *15*, 4928–4931; b) R. Tejero, A. Ponce, J. Adrio, J. C. Carretero, *Chem. Commun.* **2013**, *49*, 10406–10408.
- [9] T. Okino, Y. Hoashi, Y. Takemoto, *J. Am. Chem. Soc.* **2003**, *125*, 12672–12673.
- [10] J.-F. Bai, L.-L. Wang, L. Peng, Y.-L. Guo, J.-N. Ming, F.-Y. Wang, X.-Y. Xu, L.-X. Wang, *Eur. J. Org. Chem.* **2011**, 4472–4478.
- [11] a) A. M. F. Phillips, M. H. G. Pechtl, A. J. L. Pombeiro, *Catalysts* **2021**, *11*, 569; b) Z. Li, X. Li, J.-P. Cheng, *Synlett* **2019**, *30*, 1940–1949; c) X. Li, H. Deng, B. Zhang, J. Li, L. Zhang, S. Luo, J.-P. Cheng, *Chem. Eur. J.* **2010**, *16*, 450–455.
- [12] a) J. Chai, M. Head-Gordon, *Phys. Chem. Chem. Phys.* **2008**, *10*, 6615–6620; b) F. Jensen, *J. Chem. Theory Comput.* **2014**, *10*, 1074–1085; c) A. V. Marenich, C. J. Cramer, D. G. Truhlar, *J. Phys. Chem. B* **2009**, *113*, 6378–6396.
- [13] a) C. Adamo, V. Barone, *J. Chem. Phys.* **1999**, *110*, 6158–6170; b) M. Ernzerhof, G. E. Scuseria, *J. Chem. Phys.* **1999**, *110*, 5029–5036; c) P. C. Hariharan, J. A. Pople, *Theor. Chim. Acta* **1973**, *28*, 213–222; d) S. Grimme, J. Antony, S. Ehrlich, H. Krieg, *J. Chem. Phys.* **2010**, *132*, 154104; e) S. Grimme, S. Ehrlich, L. Goerigk, *J. Comput. Chem.* **2011**, *32*, 1456–1465.
- [14] See Supporting Information for full citation. a) Gaussian 09, Revision C.01, M. J. Frisch et al., Gaussian, Inc., Wallingford

- CT, 2016; b) Gaussian16, Revision B.01, M. J. Frisch et al., Gaussian, Inc., Wallingford CT, 2016; c) The 3D geometries in the manuscript were generated using CYL view20, C. Y. Legault, Université de Sherbrooke, 2020 (<http://www.cylview.org>).
- [15] Selected papers for Michael-addition using Takemoto catalysts, see: a) J. R. Pliego, Jr., *Phys. Chem. Chem. Phys.* **2020**, *22*, 11529–11536; b) T. Azuma, Y. Kobayashi, K. Sakata, T. Sasamori, N. Tokitoh, Y. Takemoto, *J. Org. Chem.* **2014**, *79*, 1805–1817; c) A. Quintard, D. Cheshmedzhieva, M. S. Duque, A. Gaudel-Siri, J.-V. Naubron, Y. Génisson, J.-C. Plaquevent, X. Bugaut, J. Rodriguez, T. Constantieux, *Chem. Eur. J.* **2015**, *21*, 778–790; d) X. Li, Y.-Y. Zhang, X.-S. Xue, J.-L. Jin, B.-X. Tan, C. Liu, N. Dong, J.-P. Cheng, *Eur. J. Org. Chem.* **2012**, 1774–1782; e) J. A. Izzo, Y. Myshchuk, J. S. Hirschi, M. J. Vetticatt, *Org. Biomol. Chem.* **2019**, *17*, 3934–3939; f) T. Okino, Y. Hoashi, T. Furukawa, X. N. Xu, Y. Takemoto, *J. Am. Chem. Soc.* **2005**, *127*, 119–125.
- [16] For selected computational papers for cycloadditions using Takemoto catalysts, see: a) F. Esteban, W. Cieslik, E. M. Arpa, A. Guerrero-Corella, S. Díaz-Tendero, J. Perles, J. A. Fernandez-Salas, A. Fraile, J. Alemañ, *ACS Catal.* **2018**, *8*, 1884–1890; b) X. Chen, Z.-H. Qi, S.-Y. Zhang, L.-P. Kong, Y. Wang, X.-W. Wang, *Org. Lett.* **2015**, *17*, 42–45.
- [17] a) A. Hamza, G. Schubert, T. Soós, I. Pápai, *J. Am. Chem. Soc.* **2006**, *128*, 13151–13160; b) E. Badiola, B. Fiser, E. Gómez-Bengoa, A. Mielgo, I. Olaizola, I. Urruzuno, J. M. García, J. M. Odriozola, J. Razkin, M. Oiarbide, C. Palomo, *J. Am. Chem. Soc.* **2014**, *136*, 17869–17881; c) J. Guo, M. W. Wong, *J. Org. Chem.* **2017**, *82*, 4362–4368.
- [18] a) T. Lu, F. Chen, *J. Comput. Chem.* **2012**, *33*, 580–592; b) W. Humphrey, A. Dalke, K. Schulten, *J. Mol. Graphics* **1996**, *14*, 33–38.

Manuscript received: April 26, 2022

Accepted manuscript online: May 17, 2022

Version of record online: May 31, 2022